

A COMPREHENSIVE MODEL FOR THE AMPLIFICATION OF ACOUSTIC PRESSURE WAVES BY SINGLE HOLE ORIFICES

P. Moussou & Ph. Testud
LaMSID UMR CNRS EDF 2832, Clamart, France

Y. Auregan
LAUM, Le Mans, France

A. Hirschberg
TUE Eindhoven, The Netherlands

ABSTRACT

Using a parallel flow approximation, a simple model of hydrodynamic instability is proposed for describing the behavior of an orifice as an acoustic amplifier. It is shown that the growing of perturbations in the vena contracta can generate negative damping for Strouhal numbers of the order of 0.2-0.5. Experimental data are provided to support the modelization: a qualitative agreement is obtained.

1. INTRODUCTION

In the past years, only a few articles have been dedicated to the whistling of orifices in pipes due to acoustic feedback (Anderson, 1953, 1954; Blake and Powell, 1986; Rienstra and Hirschberg, 2003). Some industrial studies involving cavitation have also been reported (Sato and Saito, 2001; Moussou et al., 2003; Janzen and Smith, 2004; Testud et al., 2007).

Recently, Aurégan and Starobinsky (1999) have proposed a theoretical criterion to evaluate the whistling ability of a pressure drop device, based on the determination of its scattering matrix and on the acoustic power balance in the presence of incipient pressure waves. The criterion was experimentally validated for orifices submitted to plane acoustic waves by Testud (2006). A simplification of the criterion valid for low Mach numbers was proposed by Moussou et al. (2007). It stipulates that the behaviour of an orifice can be described by a unique pressure drop coefficient function of the frequency, and the whistling ability appears for frequencies exhibiting negative damping:

$$\text{Real} \left(\frac{\Delta p}{\rho U u} \right) < 0, \quad (1)$$

where Δp is the harmonic pressure difference across the orifice, ρ is the fluid density, U is the steady fluid velocity in the vena contracta and u is the harmonic fluid velocity in the vena contracta.

2. OUTLINE OF THE APPROACH

The goal of the present paper is to physically understand the negative damping effect in (1). Having in mind that hydrodynamic instability is at stake in the high velocity area, a double expansion orifice was built up in such a way that a parallel flow approach would fairly describe the flow dynamics. The orifice is reproduced in Fig. 1. It consists out of a first expansion with a radius R and a smooth profile ensuring flow separation at the end edge, followed by an abrupt expansion with a thickness T and a radius R_{out} . An unstable shear flow is generated in this second expansion, and one expects acoustic amplification to occur there. T is equal to 10 mm, R is equal to 5 mm, R_{out} is equal to 7.5 mm. The test rig description and the experimental procedure can be found in Moussou et al. (2007). Due to lack of space, the details cannot be given here. Be it sufficient here to mention that experiments were performed with a 30 mm diameter air rig, and a fully automated acoustic pressure waves measurement system.

The orifice of Fig. 1 is modelized as follows: the unperturbed flow pattern consists of an inside area with a uniform velocity equal to U and an outside area with a vanishing velocity: this part of the orifice is called *vena contracta* in the followings, for it constitutes an idealization of the actual vena contracta in a conventional orifice. Such an abrupt shear flow is used in classical textbooks to describe the Kelvin-Helmholtz instability (Batchelor, 1967; Drazin and Reid, 1981). In

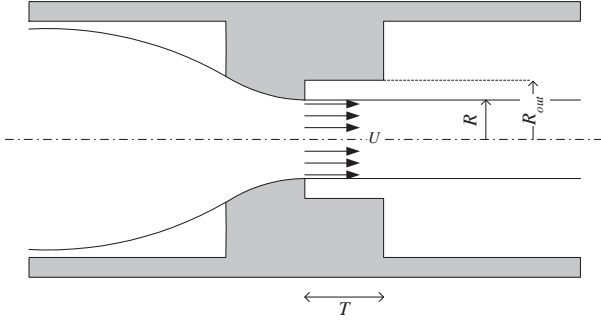


Figure 1: Sketch of the orifice

order to highlight the physical mechanisms of instability and of hydrodynamic amplification, the simple case of an ideal and inviscid flow is considered. Neither turbulence nor compressibility are taken into account, two-dimensional perturbations only are considered, and the influence of the velocity profile in the transition area is not investigated either. What is more, the amplification is assumed to be due to hydrodynamic instability in the vena contracta only, the other parts of the orifice being prone to dissipation and to inertial effects only.

Such a simplified approach cannot accurately predict the amplitude and phase of the acoustic amplification coefficients, yet it makes a physical understanding of the experimental observation possible, which is what really matters at this point. More elaborate models based on hydrodynamic modes and acoustic modes have recently been investigated (Testud, 2006; Kooijman et al., 2007), and they provide more accurate results than the ones described hereafter.

3. ORIFICE MODELIZATION

3.1. Perturbations of the parallel flow

It is assumed that growing two-dimensional perturbations are inevitably potential, so that the evolution of linear perturbations can be described by the Bernoulli equation in the inside area:

$$\frac{\partial \pi_{in}}{\partial t} + \frac{p_{in}}{\rho} + U \frac{\partial \pi_{in}}{\partial z} = 0, \quad (2)$$

and in the outside area:

$$\frac{\partial \pi_{out}}{\partial t} + \frac{p_{out}}{\rho} = 0, \quad (3)$$

where p_{in} and p_{out} are the pressures in the inside and the outside areas respectively, and where

the velocities in each half space are the gradients of the potential functions $\pi_{in}(r, z, t)$ and $\pi_{out}(r, z, t)$. Strictly speaking, the above expressions are not equal to zero but to uniform values. As a uniform term can be added to a potential π without altering the value of the corresponding velocity, these constant values can be dropped without consequences.

Equating the values of the pressure on each side of the vortex sheet, one gets the dynamic equation driving the evolution of the potential functions:

$$\frac{\partial \pi_{in}}{\partial t} + U \frac{\partial \pi_{in}}{\partial z} = \frac{\partial \pi_{out}}{\partial t}. \quad (4)$$

Mass conservation is locally ensured by the vanishing of the Laplacians of π_{in} and π_{out} , whereas the mass conservation between the two areas is obtained by introducing the vortex sheet position $\zeta(z, t)$ and by balancing the mass flux between the interface and the radius R . A straightforward calculation (Drazin and Reid, 1981) brings out:

$$\frac{\partial \zeta}{\partial t} + U \frac{\partial \zeta}{\partial z} = \frac{\partial \pi_{in}}{\partial r}, \quad (5)$$

$$\frac{\partial \zeta}{\partial t} = \frac{\partial \pi_{out}}{\partial r}, \quad (6)$$

Rearranging (5) and (6), the time derivative of the vortex sheet position can be removed:

$$U \frac{\partial \zeta}{\partial z} = \frac{\partial (\pi_{in} - \pi_{out})}{\partial r}, \quad (7)$$

and one gets by eliminating ζ :

$$U \frac{\partial^2 \pi_{out}}{\partial r \partial z} = \frac{\partial^2}{\partial r \partial t} (\pi_{in} - \pi_{out}). \quad (8)$$

The next simplifying assumption consists of separating the variables in the potential functions, as classically done in parallel flow studies (Huerre and Monkewitz, 1990; Michalke, 1965). Let the velocity flow be derived on each half space from a potential function, equal to the product of a function of time and of the abscissa $f(z, t)$ and of a function of the radial coordinate $g(r)$. The fluid incompressibility condition is:

$$\frac{\partial^2 f}{\partial z^2} = k^2 f \quad \text{and} \quad \frac{d}{dr} r \frac{dg}{dr} = -k^2 r g \quad (9)$$

where k is a constant with the dimensions of a wavenumber. The solution of the first equation is a combination of terms $h(t)e^{\pm kz}$, and the solution of the second one is a combination of Bessel

functions $J_0(\pm kr)$ and $Y_0(\pm kr)$. As indicated in sections 9.1.35 and 9.1.36 of Abramowitz and Stegun (1964), the functions $J_0(-kr)$ and $Y_0(-kr)$ are linear combinations of $J_0(kr)$ and $Y_0(kr)$ so that only two out of four terms are required. Let then the solutions of (9) be written in harmonic regime:

$$\pi_{in} = a_k e^{kz} \Phi_{in}(kr) \quad (10)$$

$$\pi_{out} = b_k e^{kz} \Phi_{out}(kr) \quad (11)$$

where the time dependence $e^{j\omega t}$ is understated, where a_k and b_k is a couple of complex amplitude terms, and where Φ_{in} and Φ_{out} are the combinations of Bessel functions complying with the boundary conditions of the inner cylinder and of the outer cylinder respectively, with a normalisation such that $\Phi_{in}(kR)$ and $\Phi_{out}(kR)$ are both equal to unity. Demanding the velocity not to diverge along the axis of the cylinder, and demanding the radial velocity vanish at the outer radius, and using the fact that $J'_0(Z) = -J_1(Z)$ and $Y'_0(Z) = -Y_1(Z)$ (Abramowitz and Stegun, 1964), one gets:

$$\Phi_{in}(kr) = \frac{J_0(kr)}{J_0(kR)} \quad (12)$$

$$\Phi_{out}(kr) = \frac{Y_1(kR_{out})J_0(kr) - J_1(kR_{out})Y_0(kr)}{Y_1(kR_{out})J_0(kR) - J_1(kR_{out})Y_0(kR)} \quad (13)$$

3.2. Dispersion relations

From now on, the discussion is focused on harmonic regimes, and an expression of the wavenumber as a function of the circular frequency is needed. Replacing the time derivative by a multiplication by $j\omega$ and introducing (10) and (11) into (4), one gets:

$$(j\omega + kU)a_k = j\omega b_k \quad (14)$$

Denoting $\epsilon = \sqrt{\frac{\Phi'_{in}(kR)}{\Phi'_{out}(kR)}}$ and introducing (10) and (11) into (8), one gets:

$$(j\omega + kU)b_k = \epsilon^2 j\omega a_k \quad (15)$$

Solving the eigenvalue problem (14) and (15), one gets a couple of dispersion relations

$$j\omega_{\pm} = \frac{-kU}{1 \mp \epsilon} \quad (16)$$

The eigenfrequencies ω_{\pm} are associated with velocity fields which are gradients of the potential functions:

$$\pi_{in} = A_k \Phi_{in}(kr) e^{kz} \quad (17)$$

$$\pi_{out} = \pm \epsilon A_k \Phi_{out}(kr) e^{kz} \quad (18)$$

where A_k is a complex amplitude.

3.3. Mass flow in the vena contracta

The issue is now to describe the average velocity generated by a perturbation in the vena contracta in harmonic regime. Let the abscissa range from 0 to T , and let k be one of the wavenumbers associated with the current circular frequency. Let q_{in} and q_{out} be the mass flows associated with the perturbation in the inside and the outside areas respectively. Derivating the potentials (17) and (18) with respect to z , the mass flows can be expressed as:

$$q_{in} = 2\pi\rho \int_0^{R+\zeta} r(k\pi_{in} + U)dr - \pi\rho R^2 U \quad (19)$$

$$q_{out} = 2\pi\rho \int_{R+\zeta}^{R_{out}} r k \pi_{out} dr \quad (20)$$

The integral terms in the above equations can be simplified by noting, first, that at the lower order, the cross products $\zeta\pi$ vanish, second, that as the radial components of the potentials are combinations of Bessel functions of order zero, the r.h.s. term of Eq. (9) can be used to perform partial integrations, and third that the radial velocity vanishes at radii 0 and R_{out} , so that one finally gets:

$$q_{in} = 2\pi\rho R \left(\zeta U - \frac{1}{k} \frac{\partial \pi_{in}}{\partial r}(kR) \right) \quad (21)$$

$$q_{out} = 2\pi\rho R \frac{1}{k} \frac{\partial \pi_{out}}{\partial r}(kR) \quad (22)$$

As could be expected from fluid incompressibility, the sum of the two above flows is independent on the abscissa z : applying Eq. (7), the derivative of the total flow with respect to z vanishes. More specifically, using (6), (16), (17) and (18), it can easily be shown that:

$$q_{in} = -q_{out} = \mp 2\pi\rho R \epsilon A_k \Phi'_{out}(kR) e^{kz} \quad (23)$$

The total mass flow vanishes for perturbations of the type described by (17) and (18). This property could be expected a priori considering Eq. (19) and (20), where all terms are proportional to e^{kz} : mass conservation demands the total mass flow be equal to zero. Yet, such a flow pattern cannot comply with the boundary condition at $z = 0$, because the axial velocity must vanish at radii higher than R , and it must convey a non-vanishing flow in the inside area. To kill two birds with one stone, one needs to add a uniform

velocity in the vena contracta. Hence, the net velocity does not vanish, the perturbation can interact with the outside system, and the boundary condition at $z = 0$ can be fulfilled. Let then the mass flows be modified by adding a uniform term to each of them:

$$q_{in} = \mp 2\pi\rho R\epsilon A_k \Phi'_{out}(kR)(e^{kz} + 1) \quad (24)$$

$$q_{out} = \pm 2\pi\rho R\epsilon A_k \Phi'_{out}(kR)(e^{kz} - 1) \quad (25)$$

and the total flow is:

$$q = \mp 4\pi\rho R\epsilon A_k \Phi'_{out}(kR) \quad (26)$$

3.4. Fluid force exerted upon the vena contracta

Let now the axial force F exerted upon the fluid in the vena contracta be expressed. First, the contribution of the pressure forces associated with the velocity fields described by (17) and (18) are determined with the help of (2) and (3). The integrals of the pressure upon the inner and outer cross sections are respectively:

$$\langle pS_{in} \rangle = -2\pi(j\omega_{\pm} + kU)\rho \int_0^{R+\zeta} r\pi_{in} dr \quad (27)$$

$$\langle pS_{out} \rangle = -2\pi j\omega_{\pm}\rho \int_{R+\zeta}^{R_{out}} r\pi_{out} dr \quad (28)$$

Proceeding as previously, one can perform partial integrations and determine the average pressure in a cross section:

$$\langle pS \rangle = \frac{2\pi R\rho}{k^2} \left((j\omega_{\pm} + kU) \frac{\partial\pi_{in}}{\partial r} - j\omega_{\pm} \frac{\partial\pi_{out}}{\partial r} \right) \quad (29)$$

the values of the potential being expressed at radius $r = R$. Using (6), (16), (17) and (18), and without taking into account the uniform flow term, it can easily be shown that the pressure force exerted upon the vena contracta can be written as:

$$F_w = \pm j\omega_{\pm} \frac{2\pi R\rho}{k} \epsilon(\epsilon^2 - 1) \Phi'_{out} A_k (1 - e^{kT}) \quad (30)$$

Adding the dynamic pressure force $j\omega Tq$ due to the uniform flow, and rearranging the first term by eliminating ω , one gets the expression of the pressure force exerted upon the vena contracta:

$$F = (1 \pm \epsilon)(e^{kT} - 1)qU + j\omega_{\pm} Tq \quad (31)$$

Eq. (31) contains in a nutshell all the amplification and phase-shifting mechanisms needed to enhance instability in an orifice.

3.5. Elaboration of an orifice model

In order to achieve a realistic description, it would be convenient to expand the velocity field in the vena contracta in k -modes, so that the axial velocity at $z = 0$ and $R < r < R_{out}$ would actually vanish (Aurégan et al., 2001). What is more, the Kutta condition at the leading edge of the first expansion should be enforced as well. In the framework of the present paper however, only one wavenumber shall be used, assuming that the contribution of higher modes is not too important, because a high value of k implies an oscillating velocity profile in the radial direction, without any noticeable contribution to the net mass flow. Let then the perturbation be associated with a velocity u in the vena contracta, such that $u = \frac{q}{\rho\pi R_{out}^2}$, and let the wavenumber k be the first solution of the dispersion relation (16) (see Appendix for details).

The behaviour of the other parts of the orifice can be described by adding a pressure drop term $\xi\rho Uu$ obtained by linearization of the usual pressure drop law (Blevins, 1992; Idelchik, 1996), and a dynamic term $j\omega L_{eq}u$ corresponding to the pressure generated by fluid acceleration through the orifice. The two coefficients ξ and L_{eq} are constant and depend on the orifice features only.

The harmonic pressure difference across the orifice is the summation of the pressure difference in the vena, obtained by dividing the force (31) by the vena surface πR_{out}^2 , and of the pressure difference upstream and downstream the vena. One gets:

$$\frac{\Delta p}{\rho U u} = (1 \pm \epsilon)(e^{kT} - 1) + \xi + \frac{j\omega_{\pm}(T + L_{eq})}{U} \quad (32)$$

Equation (32) constitutes the theoretical model of an orifice. The second term of this equation is real and positive: it describes dissipation by turbulence. The third one is imaginary and it describes inertial effects. Acoustic amplification can be generated by the first term only through hydrodynamic instability, and it occurs when this term exhibits a negative real part, i.e., negative damping.

4. EXPERIMENTAL VALIDATION AND PERSPECTIVES

As shown in Fig. 2, results are provided for three different velocities. As can be seen, the negative damping effect is lower than predicted by the model, but the general trend is roughly obtained. In the range of Strouhal numbers close to 0.2-0.5,

the real part of the generalized pressure drop coefficient become negative. The imaginary part of the coefficient exhibits a broad hump in the same range, and increases almost linearly afterwards, with an amplitude depending on the fluid velocity, as described by the $j\omega L_{eq}$ term. The experimental results do not however collapse adequately, and some further investigation is needed to clarify that point.

Differences between the model and the measurements are likely to be due, first, to the oversimplification of the model, second, to the effect of the actual velocity profile in the vena. Some further work is needed to study this last point, and the influence of air compressibility as well.

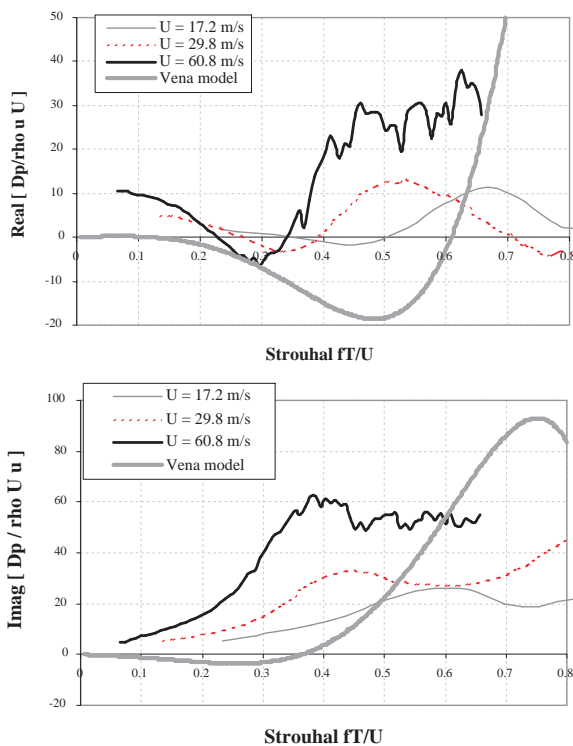


Figure 2: Comparison of experimental data and of the model of vena contracta

5. REFERENCES

Abramowitz, M. and Stegun, I. A., 1964, Handbook of Mathematical functions with formulas, graphs and mathematical tables *Applied Mathematics Series*, 55 (ed. National Bureau of Standard).

Anderson, A. B. C., 1953 A circular-orifice number describing dependency of primary Pfeifen-

ton frequency on differential pressure, gas density and orifice geometry *J. Acoust. Soc. Am.* **25**: 626-631.

Anderson, A. B. C., 1954, A jet-tone orifice number for orifices of small thickness-diameter ratio *J. Acoust. Soc. Am.*, 25, 21-25.

Aurégan, Y., Starobinski, R., 1999 Determination of acoustic energy dissipation/production potentiality from the acoustic transfer of a multipoint *Acustica*, 85, 788-792

Aurégan, Y., Debray A., Starobinski R. 2001 Low frequency sound propagation in a coaxial cylindrical duct: application to sudden area expansions and to dissipative silencers *Journal of Sound and Vibration* 243 **3**: 461-473

Batchelor, G. K., 1967, An Introduction To Fluid Dynamics (ed. Cambridge Math. Library).

Blake, W., K., Powell, A., 1986 The development of contemporary views of flow-tone generation Vol. 1, Academic Press, Orlando

Blevins, R. D., 1992 Applied Fluid Dynamics Handbook Krieger Publ. Comp., Malabar, Florida

Drazin, P. G. and Reid, W. H., 1981, Hydrodynamic Instability (ed. Cambridge Univ. Press).

Huerre, P. and Monkewitz, P. A., 1990, Local and global instabilities in spatially developing flows. *Annual Review of Fluid Mechanics*, 22: 472-537

Idelchik, I.,E., 1996, Handbook of hydraulic resistance ASME Books, New York

Janzen, V. P. and Smith, B., 2004 Acoustic properties of high energy orifice assemblies in *Proc. of the 8th int. Conf. on Flow Induced Vibration* de Langre and Axisa ed., Paris

Kooijman, G., Testud, Ph., Aurégan, Y. and Hirschberg, A. Multimodal method for scattering of sound at a sudden area expansion in a duct with subsonic flow. *Journal of Sound and Vibration*, article in Press

Lamb, H. 1932 Hydrodynamics, Dover Publications

Michalke, A., 1965 On spatially growing disturbances in an inviscid shear layer *Journal of Fluid Mechanics*, 23, **3**, 521-544

Moussou, P., Caillaud, S., Villouvier, V., Archer, A., Boyer, A. Rechu, B. Benazet, B., 2003, Vortex shedding of a multi-hole orifice synchronized to an acoustic cavity in a PWR piping system PVP-Vol. 465, Flow-induced vibrations, pp. 161-168

Moussou, P., Testud, P., Aurégan, Y., Hirschberg, A., 2007, An acoustic criterion for the whistling ability of orifices in pipes Paper PVP2007-726157 in Proc. of ASME PVP 2007, San Antonio, Texas

Rienstra, S. W., Hirschberg, A., 2003 An Introduction to Acoustics, revised version of IWDE 92-06, Eindhoven University of Technology, the Netherlands

Sato, K., and Saito, Y., 2001 Unstable Cavitation Behavior in a Circular-Cylindrical Orifice Flow CAV2001 (4th Symposium on Cavitation)

Testud, P., 2006, Aeroacoustics of orifices in confined flow, whistling and cavitation Ph. D. thesis, Université du Maine, Académie de Nantes.

Testud, P., Moussou, P., Hirschberg, A. and Aurégan, Y., 2007 Noise generated by cavitating single-hole and multi-hole orifices in a water pipe *Journal of Fluids and Structures* **23** 2 : 163-189

A. DERIVATION OF THE WAVENUMBERS

It can be shown by expressing the terms φ' as functions of the radii R and R_{out} and of the wavenumber k that $\varphi'_{in}/\varphi'_{out}$ is a regular function of k and R . It can also be shown that the poles and zeros of $\varphi'_{in}/\varphi'_{out}$ are all located along the real axis, and one expects them to constitute ends of the dispersion branches when harmonic regimes are involved. What is more, the dispersion relations (16) exhibit symmetries; changing k by k^* makes ω_{\pm} become $-\omega_{\pm}^*$, $\varphi'_{in}/\varphi'_{out}$ is an even function of k , so that changing k by $-k$ makes ω_{\pm} becomes $-\omega_{\pm}$.

As regards the numerical determination of the wavenumbers generating real frequencies, some care is required to cope with the square root in Eq. (16), for it introduces a discontinuity at points where $\varphi'_{in}/\varphi'_{out}$ exhibits a real and negative value, for wavenumbers the argument of which equals $\pm\pi$. An empirical way to remove this drawback consists of modifying the definition of the square root, and to use a couple of solutions R and $-R$ defined by $R(re^{j\theta}) = \sqrt{r}e^{j\frac{\theta}{2}}$ if

$0 \leq \theta \leq \pi$ and $R(re^{j\theta}) = -\sqrt{r}e^{j\frac{\theta}{2}}$ if $-\pi \leq \theta \leq 0$. The wavenumbers associated with a real and positive frequency can then be numerically obtained. An illustration is given in Fig. 3, where the wavenumbers associated with real positive frequencies are plotted in the $Re(k) > 0$ half plane. The symmetry $k \rightarrow -k^*$ should be used to determine the corresponding points in the $Re(k) < 0$ half plane, and the symmetry $k \rightarrow -k$ should be used to determine the wavenumbers associated with real and negative frequencies.

As shown in Fig. 4, the first dispersion branch can be approximated by:

$$kR = (1 - j) \frac{\omega R}{U} \quad (33)$$

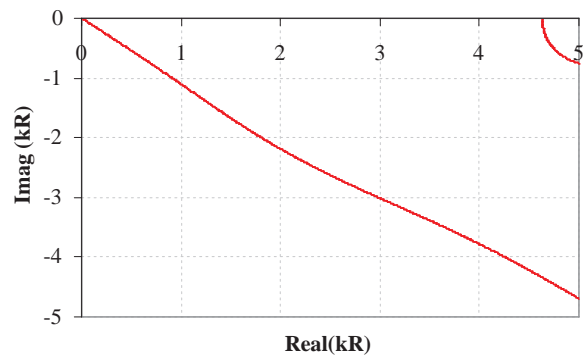


Figure 3: Loci of the wavenumbers associated with a real and positive frequency in the $Re(z) > 0$ half plane for $R/R_{out} = 0.66$

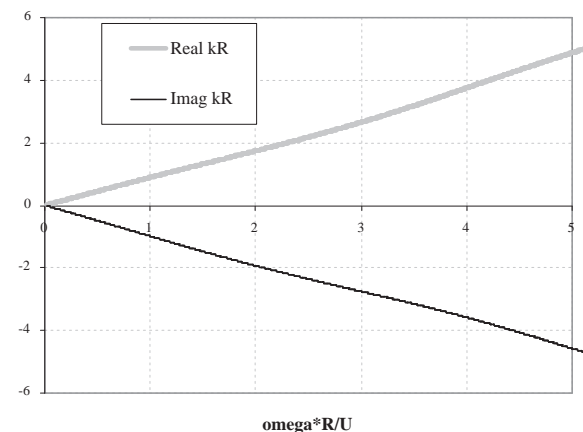


Figure 4: Real and imaginary part of kR vs. dimensionless frequency for $R/R_{out} = 0.66$